Second United Nations International Conference on the Peaceful Uses of Atomic Energy

A/CONF.15/P/2488
USA
4 August 1958

ORIGINAL: ENGLISH

Confidential until official release during Conference

OPERATIONAL CHARACTERISTICS OF THE STABILIZED TOROIDAL PINCH MACHINE, PERHAPSATRON S-4*

J. P. Conner, D. C. Hagerman, J. L. Honsaker, H. J. Karr, J. P. Mize, J. E. Osher, J. A. Phillips and E. J. Stovall, Jr.

I. INTRODUCTION

Several investigators[1-6] have reported initial success in stabilizing a pinched discharge through the utilization of an axial B_z magnetic field and conducting walls and theoretical work[7-11], with simplifying assumptions, predicts stabilization under these conditions. At Los Alamos this approach has been examined in linear (Columbus) and toroidal (Perhapsatron) geometries.

Perhapsatron S-3 (PS-3) described elsewhere[4], was found to be resistance limited in that the discharge current did not significantly increase for primary voltages over 12 kv (120 volts/cm). The minor inside diameter of this machine was small, 5.3 cm, and the onset of impurity light from wall material in the discharge occurred early in the gas current cycle. It was tentatively concluded that in the small PS-3 torus the flux of energy to the walls had reached an intolerable value. The resulting evaporation or sputtering of wall material then contaminated the discharge causing the resistance of the discharge to rise. For this reason the next in the progression of toroidal machines, Perhapsatron S-4 (PS-4) was constructed, Fig. 1.

The machine has a quartz torus, 14.0-cm minor inside diameter, 218-cm mean circumference, and wall thickness 0.6 cm. An aluminum primary, 1.25-cm thick surrounds the quartz torus with minimum spacing, $\sim$ 0.4 cm, and can be energized by 90,000 joules, 20 kv at two feed points, permitting a maximum electric field of 150 volts/cm. A two-ton iron core (laminations 0.002-inch thick) links the primary and secondary and has a rating of 0.2 volt-sec. A solenoid, 1.6 turns per cm, wound around the primary is energized by a 2400 μf capacitor at voltages up to 3 kv and produces an axial B_z magnetic field up to 4000 gauss. A split in the aluminum primary allows rapid B_z field penetration.

* Los Alamos Scientific Laboratory, University of California, Los Alamos, New Mexico

II. ELECTRICAL CHARACTERISTICS

The typical behavior of gas current and secondary voltage at 25 kv is shown in Fig. 2. The current-voltage phase relation shows that the gas current is largely inductance limited and not resistance limited as observed in PS-3. After gas breakdown ~80% of the condenser voltage appears around the secondary in agreement with the ratio of source and load inductances. The rate of rise of gas current at first is large, $\sim 1.3 \times 10^{11}$ amps/sec, until the gas current contracts to cause an increase in inductance at which time the gas current is a good approximation to a sine curve. The gas current maximum is found to rise linearly with primary voltage, Fig. 3, deviating as expected at the higher voltages because of iron core saturation.

At the discharge current maximum, the secondary voltage is not zero, and if one assumes that there is no large change of inductance, the total resistance of the discharge (R = V/I) is computed to be ~ 28 milliohms.

III. EXPERIMENTAL RESULTS

A. Neutron Production

The total average yield of neutrons is $\sim 4 \times 10^6$ per discharge at 30 kv and neutron yields as high as $\sim 10^7$ per discharge have been recorded. No circumferential asymmetry in neutron yield has been observed.

The average yield of neutrons is found to vary with pressure as shown in Fig. 4. The maximum neutron yield is found at a lower pressure (~15 μ) than with the smaller machine, PS-3 (~30 μ). The neutron yield also is observed to decrease more rapidly with increasing pressure than for PS-3 and is reduced to one-half of its maximum value at a pressure of 21.5 μ.

The dependence of the average neutron yield from PS-4 on the initial axial B_z magnetic field (Fig. 5a) exhibits a striking similarity to that reported for PS-3 with an optimum value of B_z giving the maximum yield. It is also found that the optimum value of B_z varies with the applied primary voltage as shown in Fig. 5b. Again a comparison with PS-3 can be made in that a smaller value of B_z is required in the larger machine to optimize the neutron yield for a given discharge current. It is of further interest to note that for the B_z field adjusted for optimum neutron yield at various primary voltages, the yield experiences essentially a linear rise with increasing primary voltage. These data are summarized in Fig. 6.

The average times of onset, cessation, and duration of neutron emission are shown in Fig. 7a and 7b. As the primary voltage is increased the neutrons appear earlier in time and their duration grows shorter. The onset of neutrons at a fixed B_z field may well be associated with a critical value of discharge current (~ 180 ka) so that as the more the primary voltage is increased, with the resulting increase

in the rate of rise of gas current, the earlier will this critical current be reached and neutrons emitted. The termination of the neutron burst is correlated with the appearance of radiation from wall materials. At the lower voltages (20 to 24 kv), neutron emission occurs almost symmetrically in time about the current maximum with little or no impurity light (Si II) emitted in this time interval. At the higher voltages (> 24 kv), impurity light comes in earlier with an apparent quenching of the neutrons, thus leading to shorter burst duration.

The region of emission of neutrons in the torus has been measured with a large paraffin collimator used in conjunction with a fast phosphor and photomultiplier detector. The results of the measurement are shown in Fig. 8. Within the experimental errors, the results for the horizontal and vertical scan across the minor diameter are the same, and it is concluded that the source is probably symmetric about the minor axis. From a knowledge of the resolution of the collimator, these data have been unfolded with the aid of a 704 computing machine. The results of the unfolding process, (Fig. 9,A) show that the neutrons are produced in a hollow cylinder, ~ 2 cm I.D. and ~3 cm O.D., with some contribution between 8- and 14-cm diameter. The data, however, are not inconsistent with neutrons being produced uniformly in a rod 3 cm in diameter with a small contribution between this rod and the torus wall, Fig. 9,B.

The energy distributions of the emitted neutrons have been measured in two directions tangential to the major circumference: one in the direction in which deuterons are accelerated by the induced electric field, and the other opposed. An expansion type cloud chamber, 30-cm I.D., filled with CH_4 at a pressure of 1.5 atmospheres placed one meter from the torus was used as the detector. A paraffin collimator between the cloud chamber and the torus limited the accepted neutrons to those emitted tangentially from the torus. To minimize x-ray background a 0.6-cm thick lead shield surrounded the cloud chamber. The high relative neutron yield from this machine has made it possible to obtain ~ 870 usable tracks in ~ 1600 expansions. The results with the machine operating at 27.6 kv, 1500 gauss B_z field and 12.5 μ D_2 gas pressure, are shown in Fig. 10 together with a calibration run made on a Cockcroft-Walton accelerator. It is seen that the neutron energies measured in the direction in which deuterons may be accelerated in the machine are higher than those in the opposite direction, with pronounced energy peaks at 2.59 Mev in the forward direction and 2.37 Mev in the backward direction. The widths at half maximum of the neutron energy peaks are 0.3 and 0.35 Mev and only slightly larger than that of the calibration run, ~ 0.2 Mev. These energy shifts show that the center of mass of the reacting deuterons is moving in the direction of the induced electric field with a velocity of $\sim 5 \times 10^7$ cm/sec. If the assumption is made that fast deuterons react with deuterons at rest, the peak of the neutron energy distribution implies a deuteron energy of 10 kev.

B. Magnetic Field and Pressure Distributions

The B_θ and B_z magnetic field distributions have been measured across a minor diameter of the torus in the horizontal plane. If the assumption

of symmetry of the discharge about the horizontal plane is correct, then only two components of the magnetic field, B_θ and B_z, need be measured as B_r is zero. Subsequent to these measurements, other results[12] at Los Alamos in cylindrical geometry indicate a gross bodily movement of the discharge with the resulting inference that a more detailed program of measurements including the third component (radial) in toroidal geometry is required.

The magnetic fields are measured by previously described techniques[4], and the resulting calculated j_z and j_θ current density distributions at 30 kv primary voltage and 1700 gauss B_z stabilizing field are shown in Figs. 11a and 11b, respectively. The discharge appears to be confined by the pinch field and is concentrated about the axis with little or no current near the walls after the initial pinching at about one microsecond.

The discharge current along the axis is not zero when the total secondary current passes through zero. This phenomenon has been observed in the linear discharge machine, Columbus S-4[12] and is of course due to finite velocity of diffusion of currents through the conducting medium.

Pressure and current distributions were calculated from a knowledge of the magnetic fields measured along a minor diameter of the torus. The equation used for calculating the pressures along this diameter is

$$\left[p + \frac{B^2}{8\pi}\right]_{R_1}^{R_2} = -\frac{1}{4\pi}\int_{R_1}^{R_2}\left\{\frac{2R}{R^2-A^2}B_\theta^2 + \frac{B_z^2}{R}\right\}dR + \underline{C}, \qquad (1)$$

where R is the major radius to the point under consideration, A is determined by the condition $B_\theta = 0$ at $R = A$, and the arbitrary constant $\underline{C}$ is determined at some point where the pressure is known. The quantity $(R^2-A^2)/2R$ is the minor radius of the toroidal coordinate surface through the point. The equations for the current distributions along the diameter are

$$j_z = -\frac{1}{4\pi}\left(\frac{\partial B_\theta}{\partial R} + \frac{2R}{R^2-A^2}B_\theta\right) \qquad (2)$$

and

$$j_\theta = \frac{1}{4\pi}\left(\frac{\partial B_z}{\partial R} + \frac{B_z}{R}\right) \qquad (3)$$

Typical results of the pressure calculations are shown in Fig. 12.

An examination of the pressure profiles reveals several outstanding features: (1) the center of the discharge as defined by $B_\theta = 0$ does not move appreciably during the first half cycle of gas current but is localized within less than ± 1.0 cm along the axis, (2) a pressure minimum occurs

on the axis and persists during most of the first half period. Two pressure peaks of varying amplitude are present on each side of the pressure minimum at a radius of ~ 2 cm, (3) appreciable pressures of varying amplitude are present at the inside and outside walls.

These pressure distributions were unexpected as they have not been obtained in toroidal machines heretofore. The possibility exists that the assumptions made in the derivation of Eq. 1 are not valid and a complete mapping of the fields is required. It is interesting to note, however, that one possible configuration for the radial distribution of the emitted neutrons (see Fig. 9,A) is a thin shell and that this shell is located on the pressure peaks at radius ~ 2 cm.

At least three possible explanations exist for the large pressures calculated at the walls: (1) the discharge moves bodily about the tube and large inward and outward accelerations are present as has been observed radially in the linear system[12] (the present data are not sufficiently precise at this time to make a more detailed analysis), (2) high energy runaway electrons are contributing to the pressure by their centrifugal force, or (3) errors in field measurements exist near the walls or near the probe openings in the primary shell.

C. Powered Crowbar Operation

For some conditions it has been found possible to sustain the current maximum for times as long as 30 microseconds. The current is maintained by switching an additional 24 millifarads of capacitance (1.1×10^5 joules at 3 kv) in parallel with the primary energy supply at the time of current maximum. Because of the unexpected high impedance of the discharge, the discharge current could be held constant by the crowbar bank only at the level corresponding to a total primary voltage of $\lesssim$ 14 kv. If switching takes place at current maximum with initially 7 kv and 3 kv on the primary and sustaining crowbar supplies respectively, the results shown in Fig. 13 are obtained. With an initial applied secondary voltage of ~ 13 kv, it is observed that the discharge current is held relatively constant, ~180 ka, for ~30 usec by the crowbar system.

The B_θ and B_z magnetic field distributions have been measured as a function of time with a sustained crowbar operation, and the corresponding current densities, j_z and j_θ, calculated (Fig. 14a,b). Pressure profiles have also been calculated. It is surprising that for times as long as 32 μsec after the first current maximum that the magnetic field distributions vary as little as they do. It is apparent that the axial discharge current remains separated from the walls for ~48 microseconds after initiation of discharge current.

A neutron yield of $\sim 2 \times 10^5$ per burst under normal operating conditions with 13 kv applied secondary voltage increases with crowbar operation at 13 kv to $\sim 2 \times 10^6$ per burst with duration increased up to $\lesssim$ 60 μsec (Fig. 13c). The rate of neutron emission remains relatively constant during this time. This result apparently precludes explanations of neutron production which use shocks originating by rapid rate of rise of discharge currents

or sudden applications of high voltages. It appears necessary that the neutron producing mechanism be continuous for relatively long times and that it involves no permanent breakup of the pinch structure.

During the sustained crowbar operation, a considerable amount of energy (9.0×10^2 joules per μsec) is being transferred to the discharge. No appreciable changes, however, are found during these times in the pressure distributions. The conclusion is inescapable that energy is being lost by the discharge as fast as it is being received.

D. Spectral Observations

The intensities of the deuterium D_β, and silicon, Si II (4128 Å), lines vary with time as shown in Fig. 15. The hydrogen line initially is relatively intense. Radiation from the discharge gas becomes much weaker when ionization has taken place, and then becomes very strong presumably due to the ionization of hydrogen released from the walls. The time of onset of silicon light is a function of primary voltage (Fig. 7a) and is associated with the bombardment of the walls by particles or radiation.

E. X-rays

For primary voltages above ~ 20 kv a short burst of x-rays, duration ~2 μsec, is detected outside of the aluminum primary at the start of gas current. Little or no x-ray emission of energy > 50 kev occurs during the remainder of the discharge cycle. The mean energy of the x-rays outside the aluminum primary is 68 kev as measured with film badges. With an applied primary voltage of 30 kv, a maximum x-ray energy of 0.6 Mev was determined by lead absorbers. The x-ray intensity varies widely from discharge to discharge with an average reading of ~1 mr per discharge measured with a dosimeter placed alongside the torus primary.

III. DISCUSSION

From the above data some conclusions can be drawn concerning the plasma confinement and heating in Perhapsatron S-4.

A. Electrical Resistance

In the operation of PS-4, the electrical resistance of the discharge was found to be considerably larger than expected. At the discharge current maximum (3×10^5 amperes), for example, the secondary voltage was measured to be 8.4 kv which gives from Ohm's law a total discharge impedance of 28 milliohms. From the j_z and j_θ current density distributions (Fig. 11a,b) it would appear that there are no large fluctuations in the current density distributions at the current maximum (t = 12.5 μsec) indicating that at this time there is little change in the secondary inductance and hence the voltage drop is purely resistive. The current channel diameter ~7.2 cm is also defined by the j_z distribution. With the assumption that the electric field is constant throughout the discharge we calculate a resistivity of 4.0×10^{-3} ohms-cm, 45° pitch of

the magnetic field lines, and a corresponding electron temperature of ~6 ev assuming validity of the resistivity, temperature relation $\rho = 3 \times 10^{-6}/T^{3/2}$.(13)

A second measurement of the discharge resistance is available from the performance of the discharge during the sustained crowbar operation. In this case the discharge current was held essentially constant for 30 μsec with little observed change in the j_z current distributions (Fig. 14a). The discharge current was 1.8×10^5 amperes with a secondary voltage of ~ 5.0 kv. From the foregoing crowbar operating conditions, the total discharge resistance is calculated to be ~28 milliohms in agreement with the calculation made at the higher voltages and currents. At the reduced power level required for crowbar operation the discharge remains remarkably free from impurity radiation for ~40 μsec. This enables us to reject impurities as a serious contributor to the high resistivity.

A more precise and meaningful measurement of the resistivity of the discharge can be made with the knowledge of the B_θ and B_z distributions. The electric fields and current densities parallel to the magnetic field can be calculated throughout the discharge and from these data changes in the resistivity obtained as a function of time. These calculations are now being made but no results are available at this time.

In summary, the experimental results indicate that the apparent resistivity of the discharge is large (4.0×10^{-3} ohms-cm) with a corresponding low ~ 6 ev electron temperature. It should be emphasized, however, that these calculations use the simplified Ohm's law relation for the plasma[13] ignoring, in particular, velocity terms that would exist in the presence of plasma waves or turbulent conditions.

B. Energy Balance

It is instructive to account for the energy taken from the capacitor banks during the discharge. With PS-4 operating at 15 kv, the energy deposited in the various sections of the machine at a time of 6 μsec has been calculated. The results are summarized in Table I.

Table I

1.	Initial energy in condenser bank	50,600 joules	
2.	Energy remaining in condenser bank at 6 μsec		28,200 joules
3.	Energy in external inductance		2,760 "
4.	Magnetic field energy associated with discharge, $\int B_\theta^2/8\pi \, dV + \int B_z^2/8\pi \, dV - \int B_{zo}^2/8\pi \, dV$		11,620 "
5.	Resistance losses		540 "
6.	Energy in primary inductance		300 "
	Totals	50,600 joules	43,420 joules
	Energy unaccounted for		7,180 joules

If the remaining energy, 7180 joules, were used to heat all the gas initially present in the torus a plasma temperature of ~760 ev would exist at 6 μsec in the discharge cycle. This result is clearly incompatible with the ~6-ev electron temperatures calculated from the resistivity.

The sustained crowbar operation gives us additional information as to the problem of heating the plasma. With a constant current of 1.8×10^5 amperes the secondary voltage remains essentially constant at 5.0 kv for ~30 μsec. Energy is then being transferred to the discharge at a rate of approximately $(1.8 \times 10^5)(5 \times 10^3)10^{-6} = 900$ joules per μsec. The calculated current density distributions (Fig. 14a,b) indicate that this energy is not appearing in the magnetic field since these distributions do not change appreciably during this time interval. The energy must then be deposited to the gas at a rate of 95 ev per particle per μsec. However, the calculated pressures during this time interval do not rise appreciably nor does the rate of neutron production increase as would be expected from a steadily rising temperature.

These arguments lead to the obvious conclusion that there are mechanisms at work by which energy is being continuously drained from the discharge. The magnetic probe measurements indicate that the discharge current is at least grossly confined away from the tube walls, but the experimental results demonstrate that the energy transferred to the plasma is not confined. The nature of the loss mechanism is not yet known though it is suspected that loss by escape of energetic particles across the confining magnetic field, particle acceleration by the electric field, and loss by radiation generated by plasma waves and turbulence may be contributing factors.

C. Pressure Balance Results

The pressure distributions calculated from the measured magnetic field distributions in PS-4 show, in general, a pressure maximum at a radius of ~2 cm. With a pressure minimum on the axis it can be concluded that the pressure difference between the peak pressure and the axial pressure is not a result of forces such as those produced by runaway electrons. The pressure differences between the peaks and the minima at the axis vary up to ~2.5 atmospheres with corresponding energy densities of 0.25 joules per cm^3. It is not clear whether this energy exists as gas turbulence, shock waves, plasma waves, or in thermal motion of the gas particles. If it is assumed that all the gas is confined uniformly in a rod of diameter 3.5 cm, and that an energy density of 0.25 joules/cm^3 is expended in thermal motion of the gas particles within the rod then a temperature of 220 ev is deduced from the pressure measurements. This temperature is perhaps low since considerable pressures are observed between 3.5-cm radius and the wall, which indicates that all the gas may not be confined within the 3.5-cm radius.

A temperature of 220 ev is not sufficient to explain the PS-4 neutron yield based on thermonuclear reaction considerations, although as stated

above the results of the collimated neutron observations across a minor diameter suggest that the neutrons are produced in the measured high pressure regions of the discharge.

D. Neutron Energy Distributions

The energy shifts in the neutron energy distributions described earlier in this report show conclusively that most of the neutrons are generated by reacting deuterons having a center of mass velocity of $\sim 5 \times 10^7$ cm/sec.

Two possible mechanisms representing extremes of viewpoints can be considered by which the neutrons may be produced with the observed center of mass velocity: (1) a simple acceleration process in which 10-kev deuterons, which are a small fraction of the total deuterons present in the torus, react with the remaining deuterons at rest, and (2) a streaming of deuterons of velocity 5×10^7 cm/sec reacting with each other by their relative velocities.

(1) In the acceleration process we can calculate the current of 10-kev deuterons required to produce the observed neutron yield. With an initial gas pressure of 12.5 μ and an assumed compression of ten, a deuteron current of $\sim$ 370 amperes is required to give the observed rate of neutron production of $\sim 5 \times 10^{11}$ neutrons/sec. (If a smaller compression is assumed, the current will increase inversely as the compression.) The percentage of the total number of deuterons present in the torus which would contribute to this current would be small, $\sim$ 0.02%, and the energy required to accelerate them to 10 kev quite reasonable, $\sim$ 8 joules.

Possibly the strongest argument that can be made against this process of neutron production is that the required deuteron current is too large. If conservation of momentum is to occur in the discharge, then the ratio of the deuteron and electron currents should be inversely proportional to their masses. With a total discharge current of 300 ka, the deuteron current would be only 80 amperes.

The above calculation of the required deuteron current has assumed that all the accelerated deuterons have an energy of 10 kev corresponding to the peak in the neutron energy distribution. This may well be in error since comparable numbers of lower energy deuterons may be present, which would not contribute much to the total neutron yield since the cross-section is such a rapidly rising function of energy. Unfortunately the cloud chamber data are not sufficiently precise to permit a deuteron energy distribution to be calculated.

(2) If it is assumed that deuterons are streaming parallel to the axis of the torus it can be shown that the deuterons in the gas cannot all have the indicated velocity of 5×10^7 cm/sec ($\sim$ 2.5 kev energy). To accelerate all the deuterons to this energy, a total energy of 1.2×10^4 joules is required. In the energy balance consideration discussed above, only 7.2×10^3 joules are available for translational kinetic

energy. One must then conclude that only a fraction, 60% at most, of the deuterons could cooperate in this process. A difficulty arises in that this number of deuterons traveling at a velocity of 5×10^7 cm/sec would produce a current of 6.5×10^6 amperes. In order to be consistent with the observed current and momentum conservation, the steady deuteron current must not exceed 80 amperes. The pressure distribution also establishes a limit on the maximum temperature and density which can exist. We must then conclude if hypothesis (2) is correct that in order to be consistent with current and energy balance the reaction must proceed at large relative deuteron velocities in a small fraction of the total gas. The necessarily high transient pressures which would then exist would not be observed by the present techniques. This highly localized source of neutrons receives some experimental confirmation in that during the collimated neutron measurements, at a given collimator position, the numbers of neutrons detected on successive shots frequently varies by a factor of three.

Further experiments may reveal that the models developed above are gross oversimplifications of the true mechanism for neutron production in PS-4.

E. Summary

The preceding comments may be summarized as follows,

(1) The discharge has been stabilized in a gross sense (the discharge current confined from the walls) for times ~ 48 μsec.

(2) From the measured resistivity of the discharge the electron temperature is ~ 6 ev.

(3) By some as yet unknown mechanism, energy is being lost by the discharge at a rate of ~900 joules/sec under certain operating conditions.

(4) Maximum gas pressures of ~ 2.5 atmospheres are measured during the current cycle.

(5) There is a center of mass velocity of $\sim 5 \times 10^7$ cm/sec of the reacting deuterons which produce the neutrons. The mechanism responsible for the production of these neutrons is not clear.

ACKNOWLEDGMENTS

We wish to thank J. L. Tuck for helpful discussions during the course of this work and to acknowledge the cooperation of L. C. Burkhardt and R. H. Lovberg for magnetic probe assemblies, of J. W. Mather for scientific assistance, of H. J. Longley and T. L. Jordan for assistance with the calculations, of R. S. Dike for engineering design, and of R. Holm and A. Schofield for electrical design.

REFERENCES

1. Thonemann, P. C., et al, Nature 181, 217 (1958).

2. Allen, N. L., et al, Nature 181, 222 (1958).

3. Burkhardt, L. C., and Lovberg, R. H., Nature 181, 228 (1958).

4. Honsaker, J. L., et al, Nature 181, 231 (1958).

5. Bezbachenko, A. L., et al, Atomnaya Energiya 1, No. 5, 26 (1956).

6. Colgate, S., University of California Radiation Laboratory, Livermore, California (private communication).

7. Kruskal, M., and Schwarzchild, M., Proc. Roy. Soc. A, 348, 223 (1954).

8. Kruskal, M., and Tuck, J. L., Los Alamos Scientific Laboratory Report LA-1716, Proc. Roy. Soc. (to be published).

9. Tayler, R. J., Proc. Phys. Soc. B, 70, 1049 (1957).

10. Rosenbluth, M., Los Alamos Scientific Laboratory Report LA-2030, Proc. Venice Conference (1957).

11. Shafranov, V. D., Atomnaya Energiya 5, 709 (1956).

12. Burkhardt, L. C., and Lovberg, R. H., Field Configurations and Stability Studies of a Linear Discharge, Geneva Conference (1958).

13. Spitzer, L., Physics of Fully Ionized Gases (Interscience Publishers, Inc., New York, 1956).

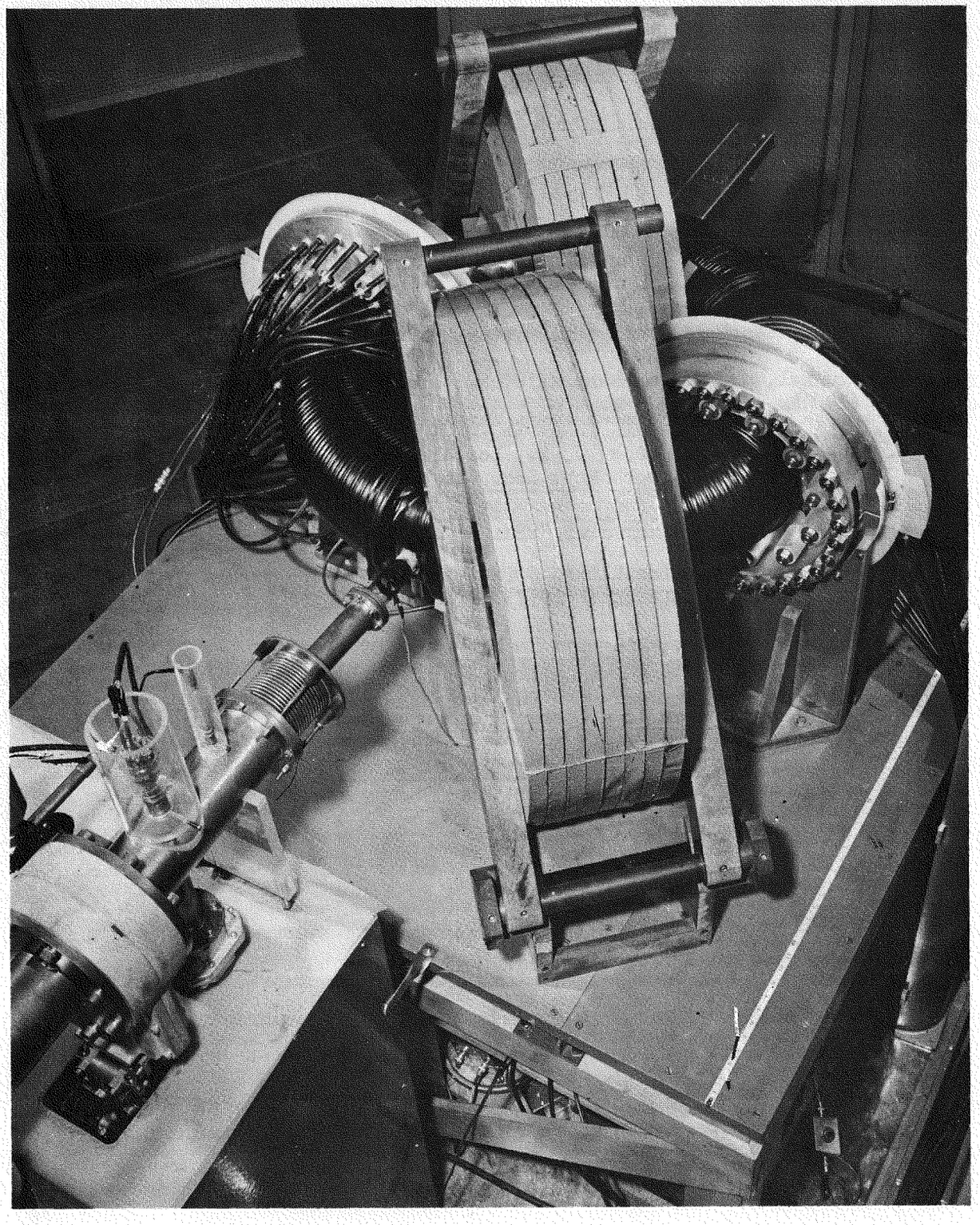

Fig. 1. Photograph of Perhapsatron S-4 showing the torus, iron cores, electrical feed points, and a section of the vacuum system.

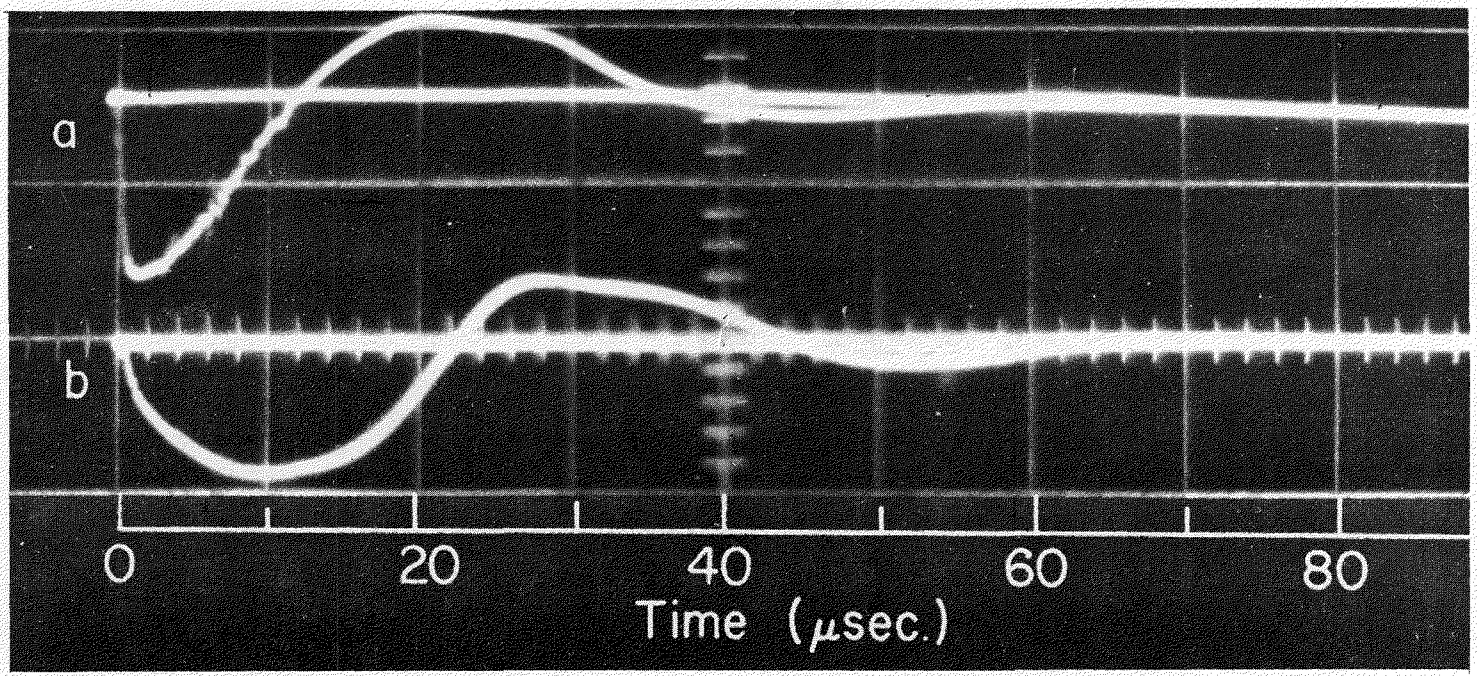

Fig. 2. Multiple beam oscilloscope traces of: (a) primary voltage; (b) gas discharge current. Initial condition: Primary voltage = 30 kv, B_z axial magnetic field = 1700 gauss, P = 12.5 microns.

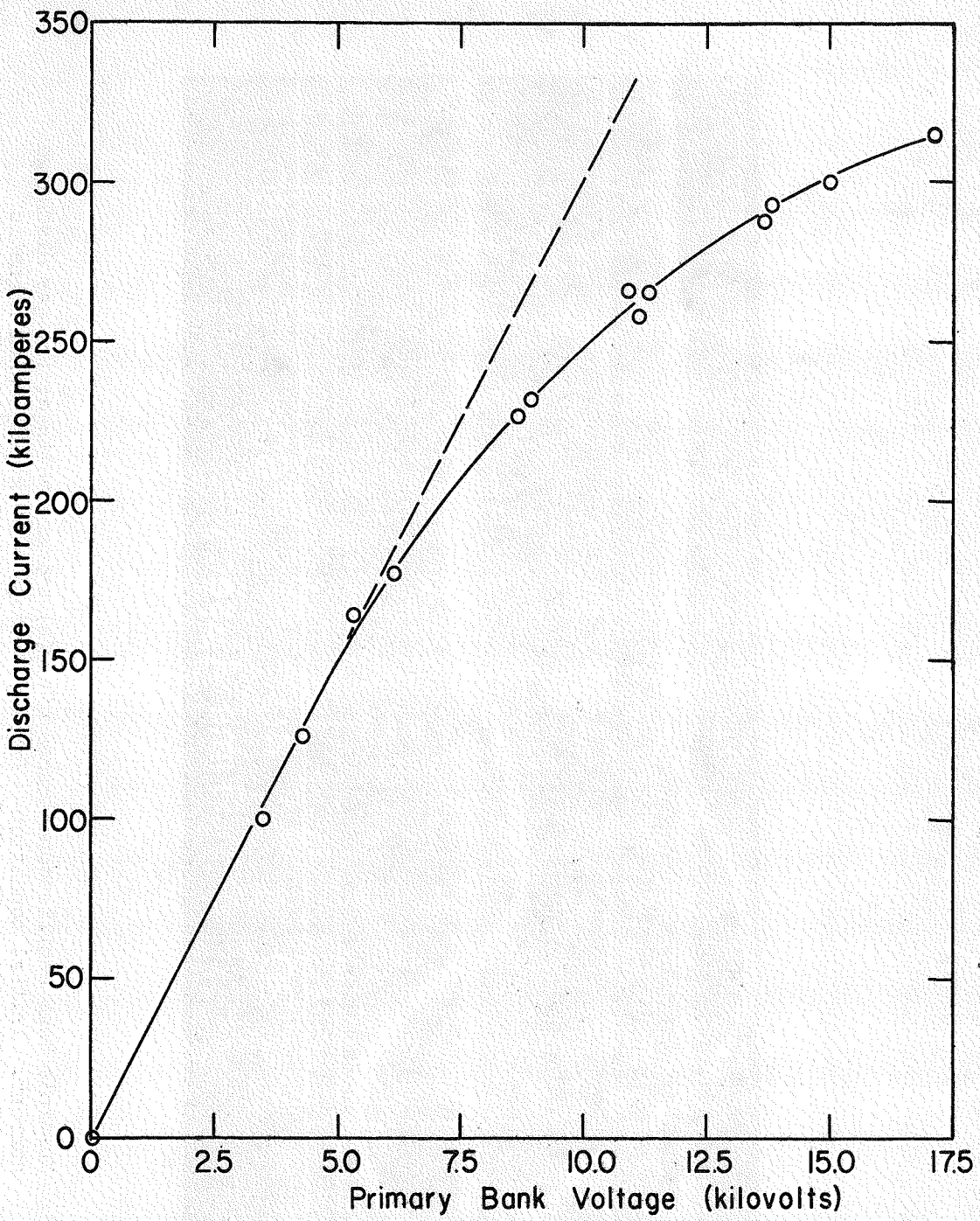

Fig. 3. Peak gas current as a function of primary voltage.

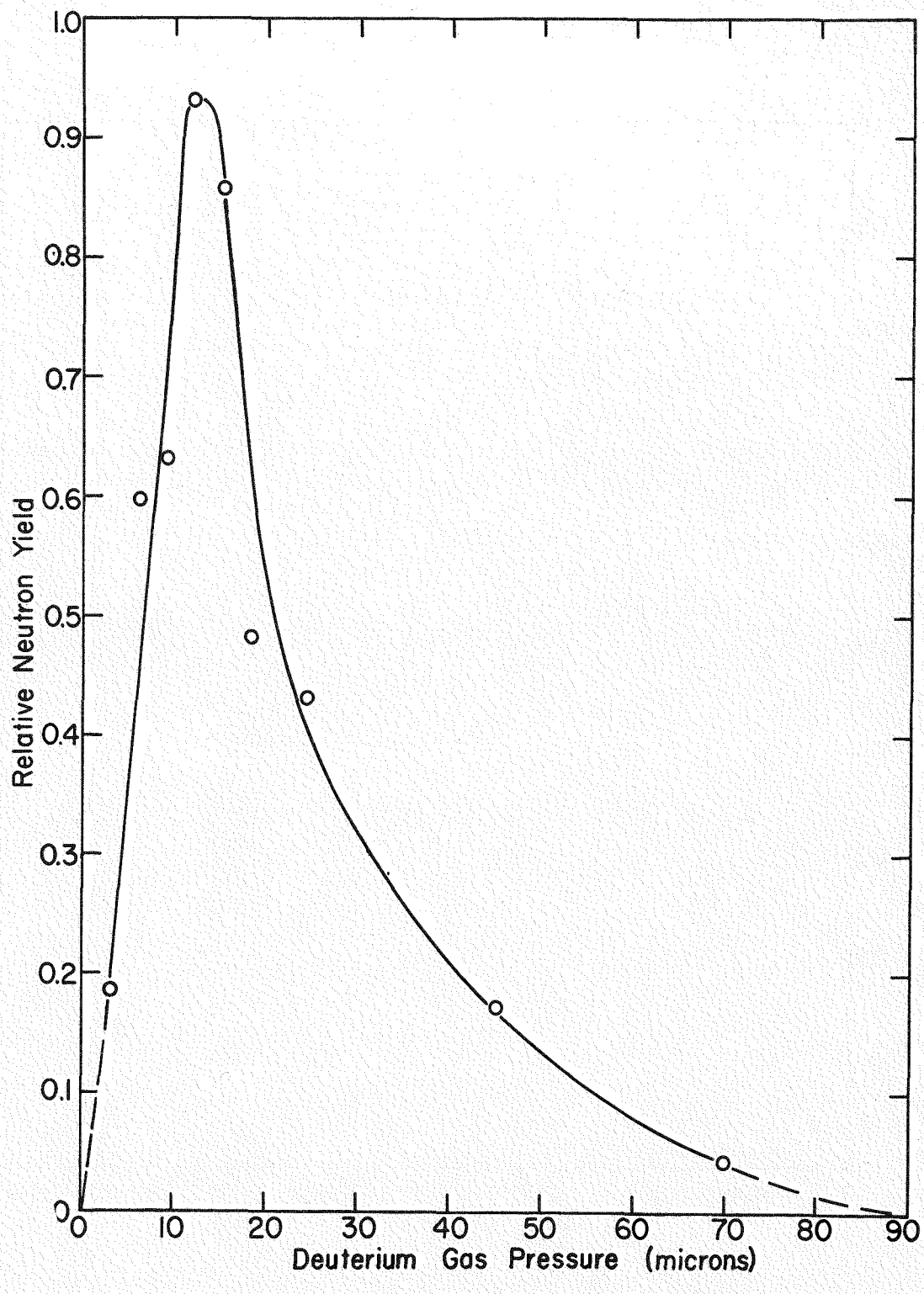

Fig. 4. Neutron yield versus deuterium gas pressure. Primary voltage = 30 kv. B_z axial magnetic field = 1700 gauss. Each point represents the average yield of 3 shots; the standard error for this average is approximately ±20%.

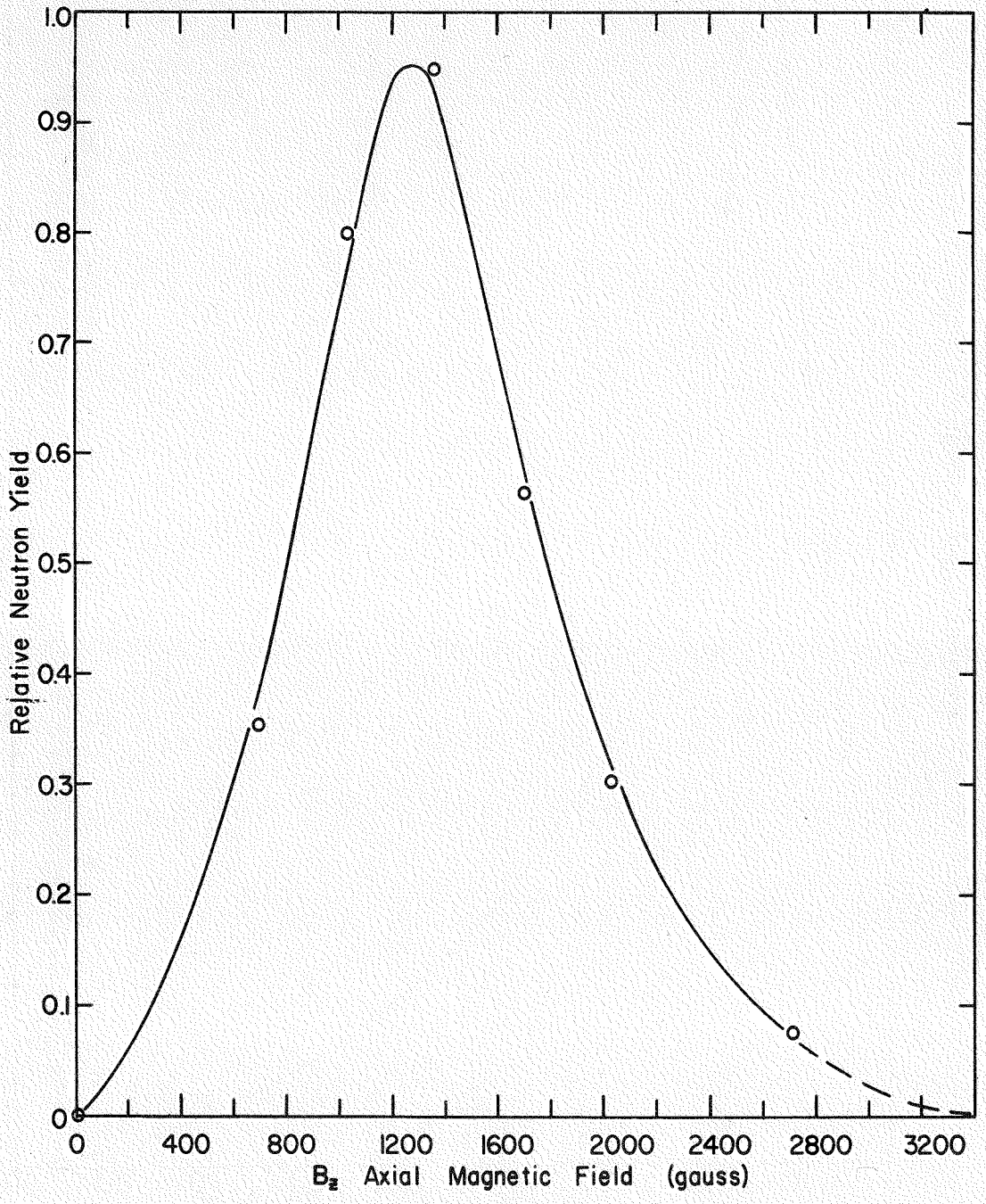

Fig. 5a. Neutron yield as a function of axial B_z magnetic field. Primary voltage = 30 kv.

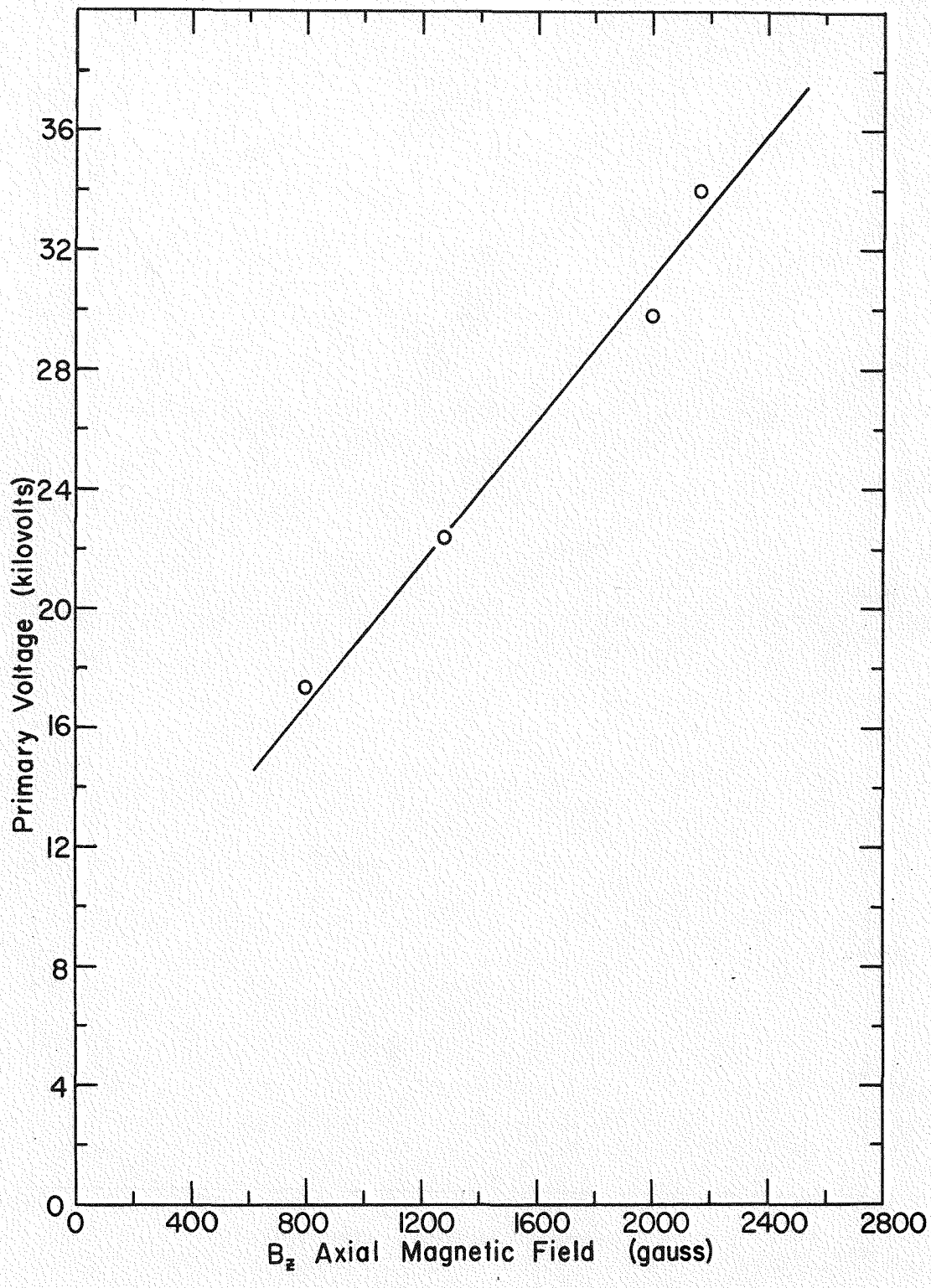

Fig. 5b. Axial B_z magnetic field for optimum neutron yield as a function of primary voltage. Deuterium gas pressure = 12.5 microns.

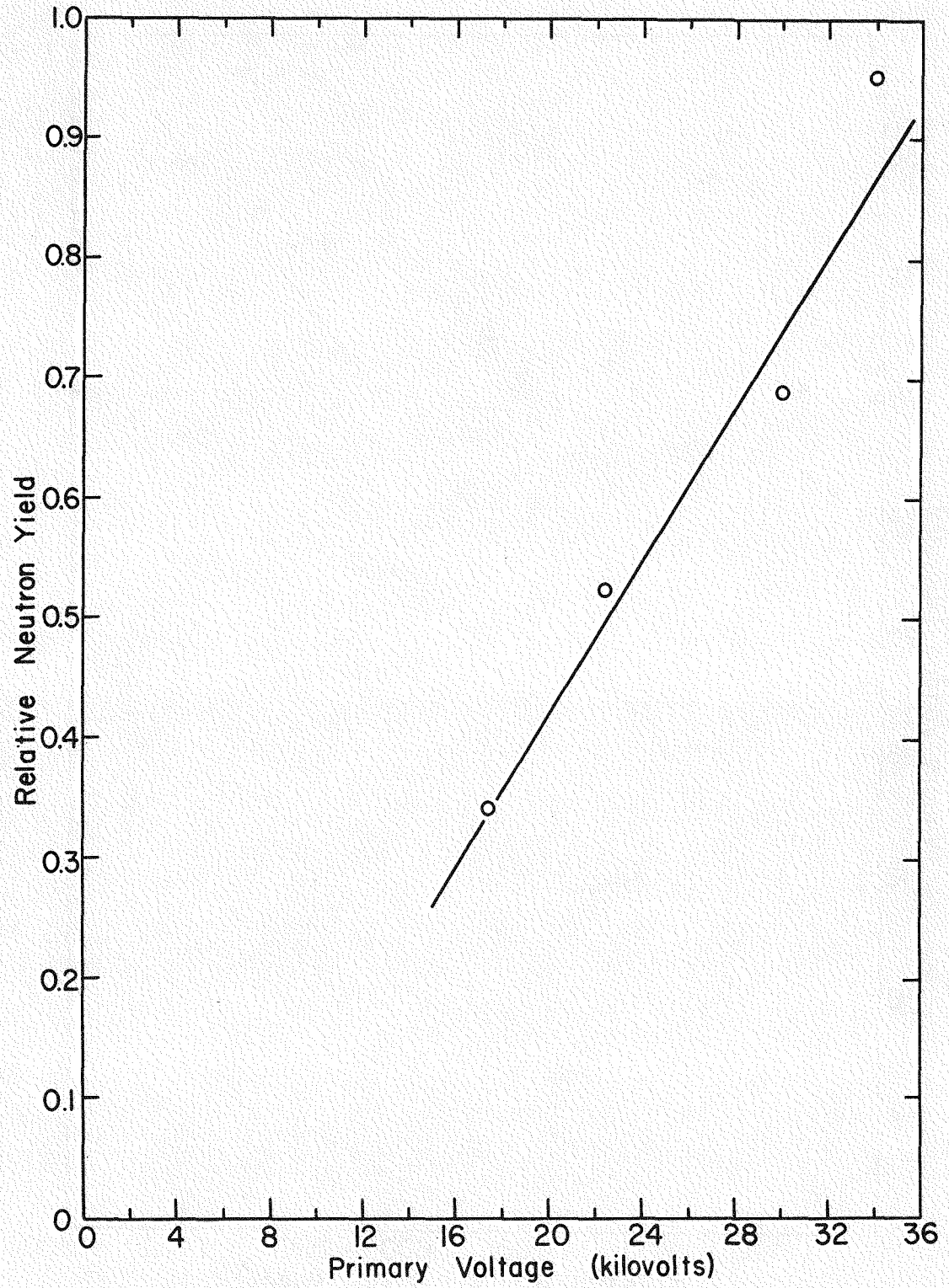

Fig. 6. Neutron yield versus primary voltage. Axial B_z magnetic field adjusted for optimum neutron yield at the individual data points. Deuterium pressure = 12.5 microns.

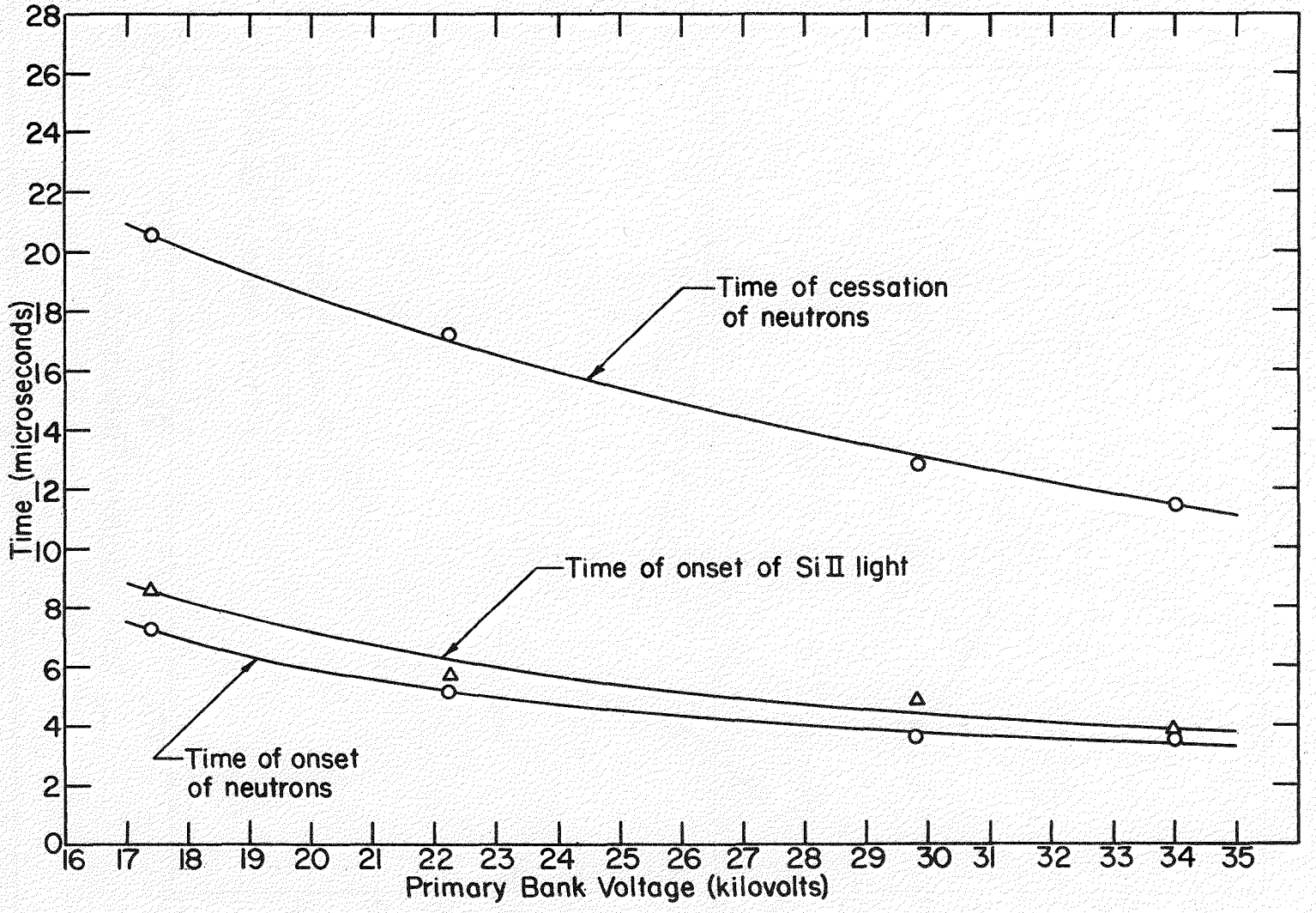

Fig. 7a. Time during gas current cycle at onset and cessation of neutrons, and time of onset of Si II 4128 Å line as a function of primary voltage. Axial B_z magnetic field adjusted for optimum neutron yield at the individual data points.

A/CONF.15/P/2488
USA

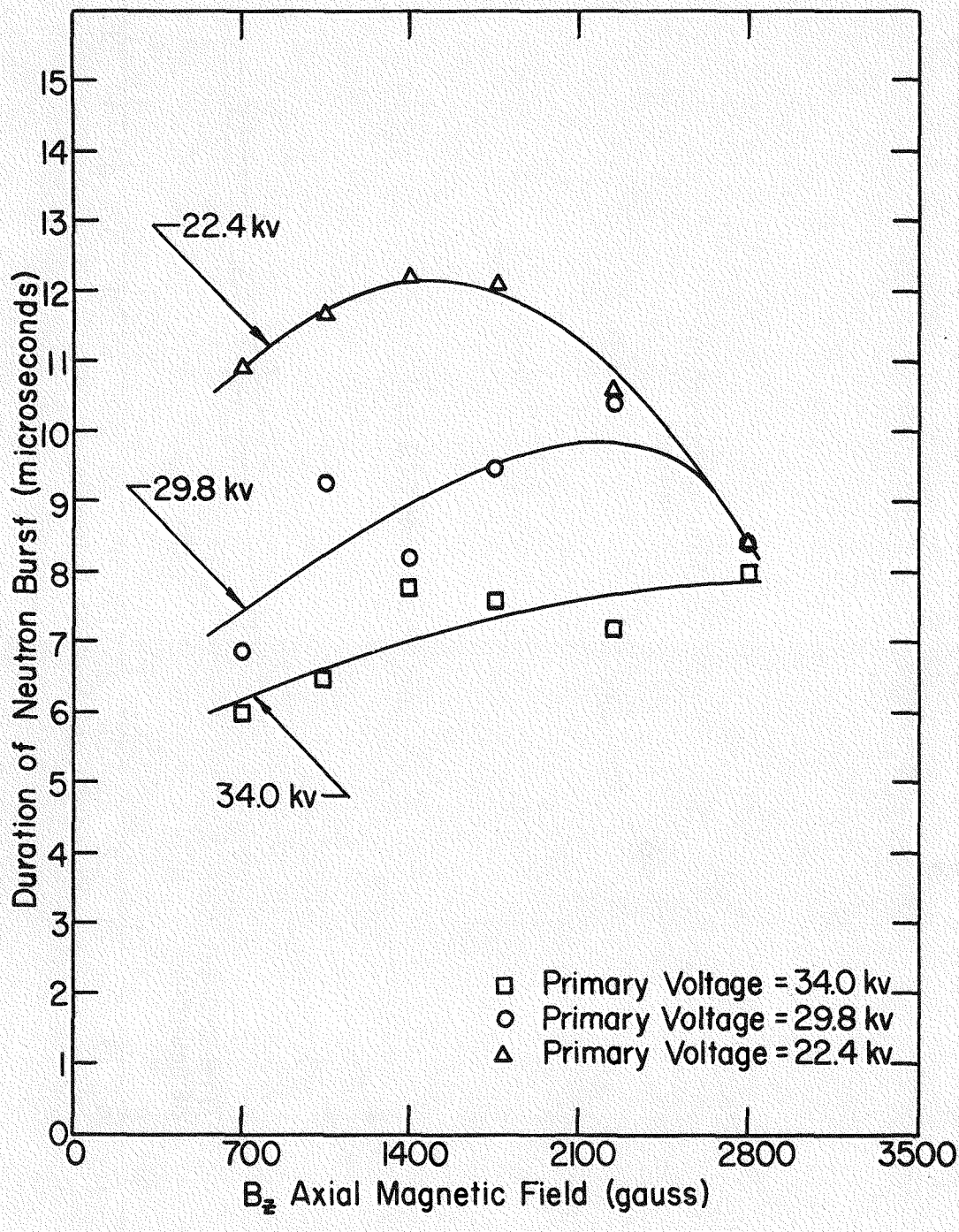

Fig. 7b. Duration of neutron burst as a function of primary voltage and axial B_z magnetic field. Deuterium gas pressure = 12.5 microns.

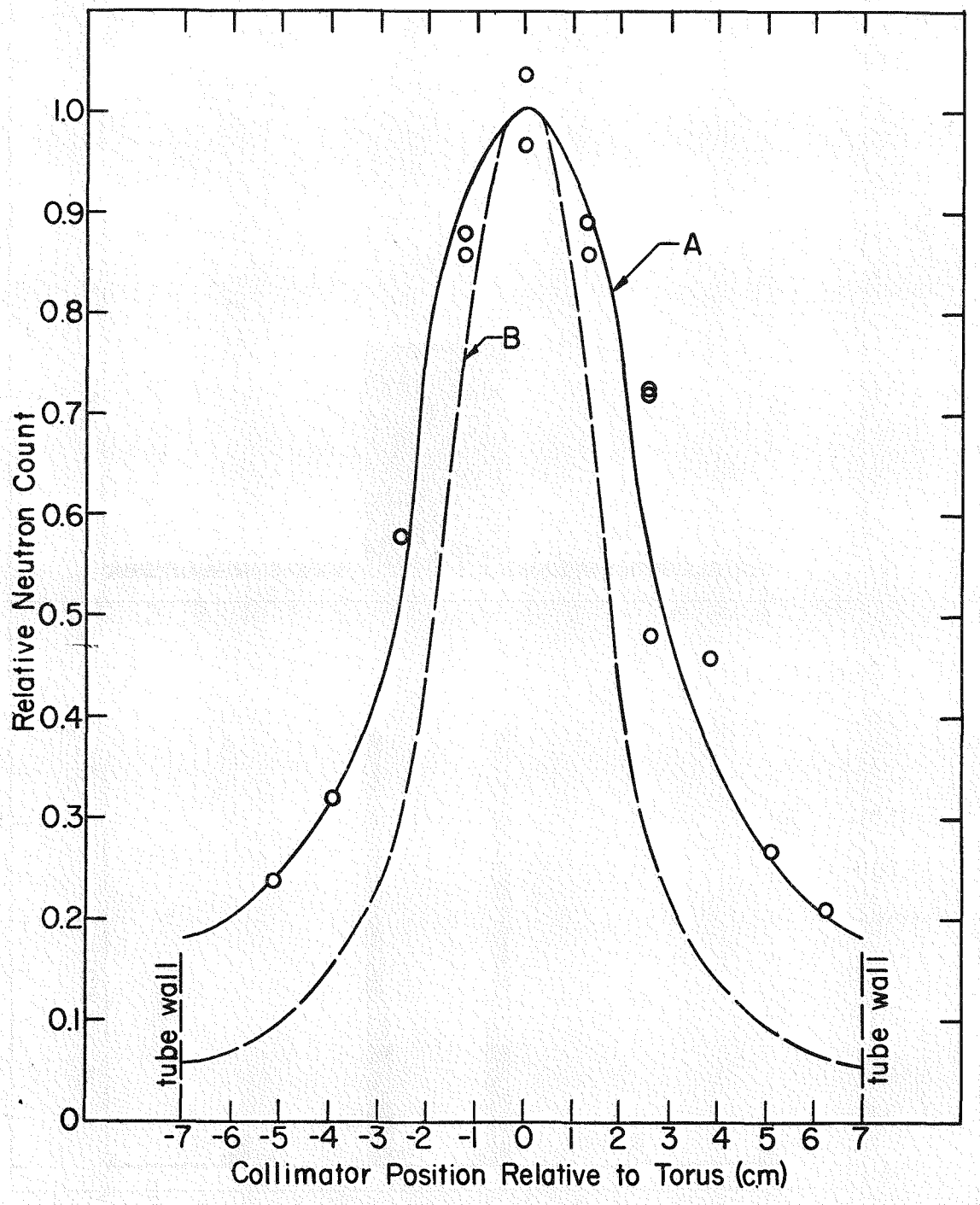

Fig. 8. Results of neutron collimation experiment, (A) vertical traverse (each data point is obtained from averaging 10 shots); (B) spatial resolution of collimated detector for a line source of neutrons from a Pu-Be source.

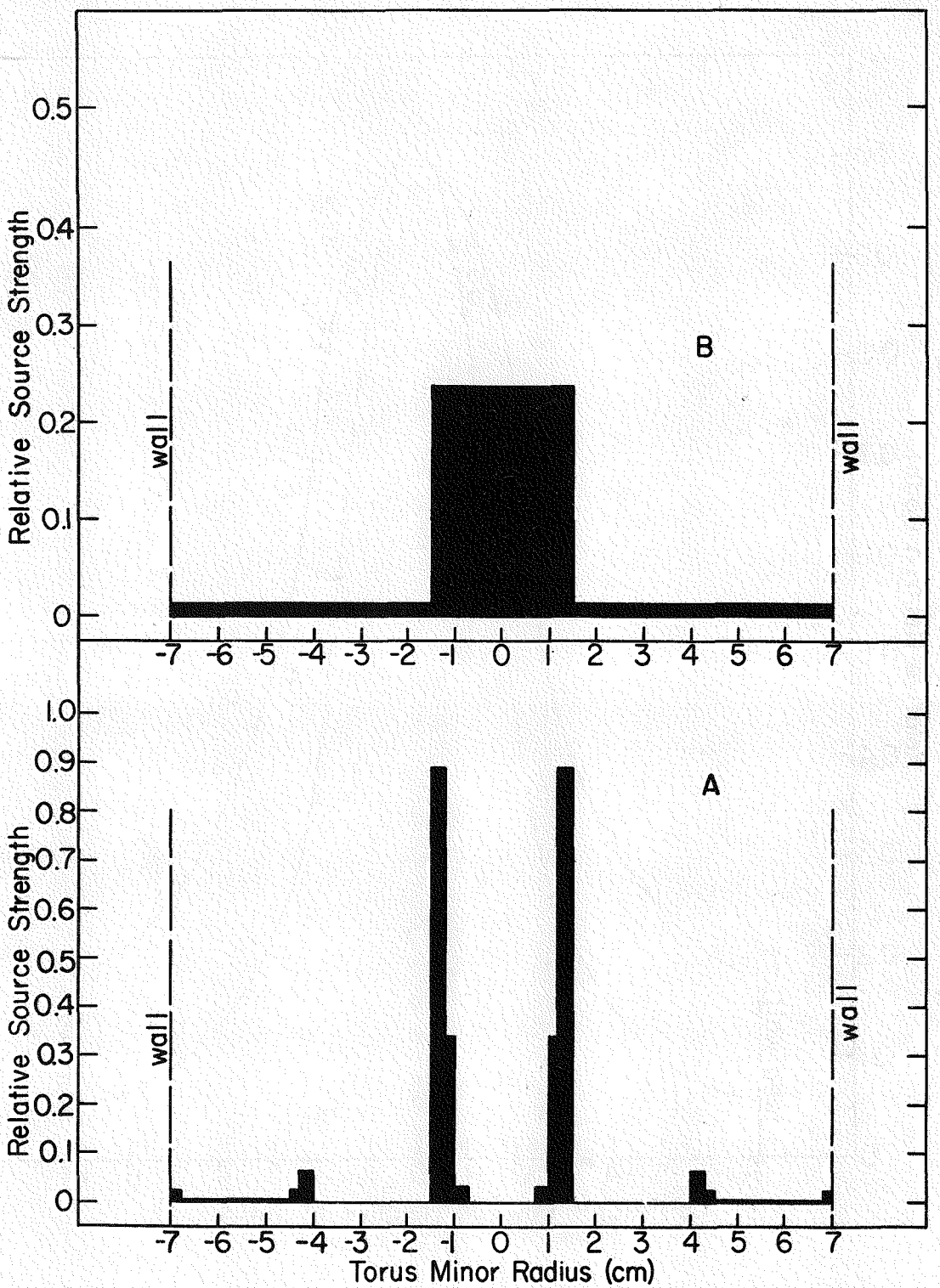

Fig. 9. Summary of analysis of experimental data presented in Fig. 8.

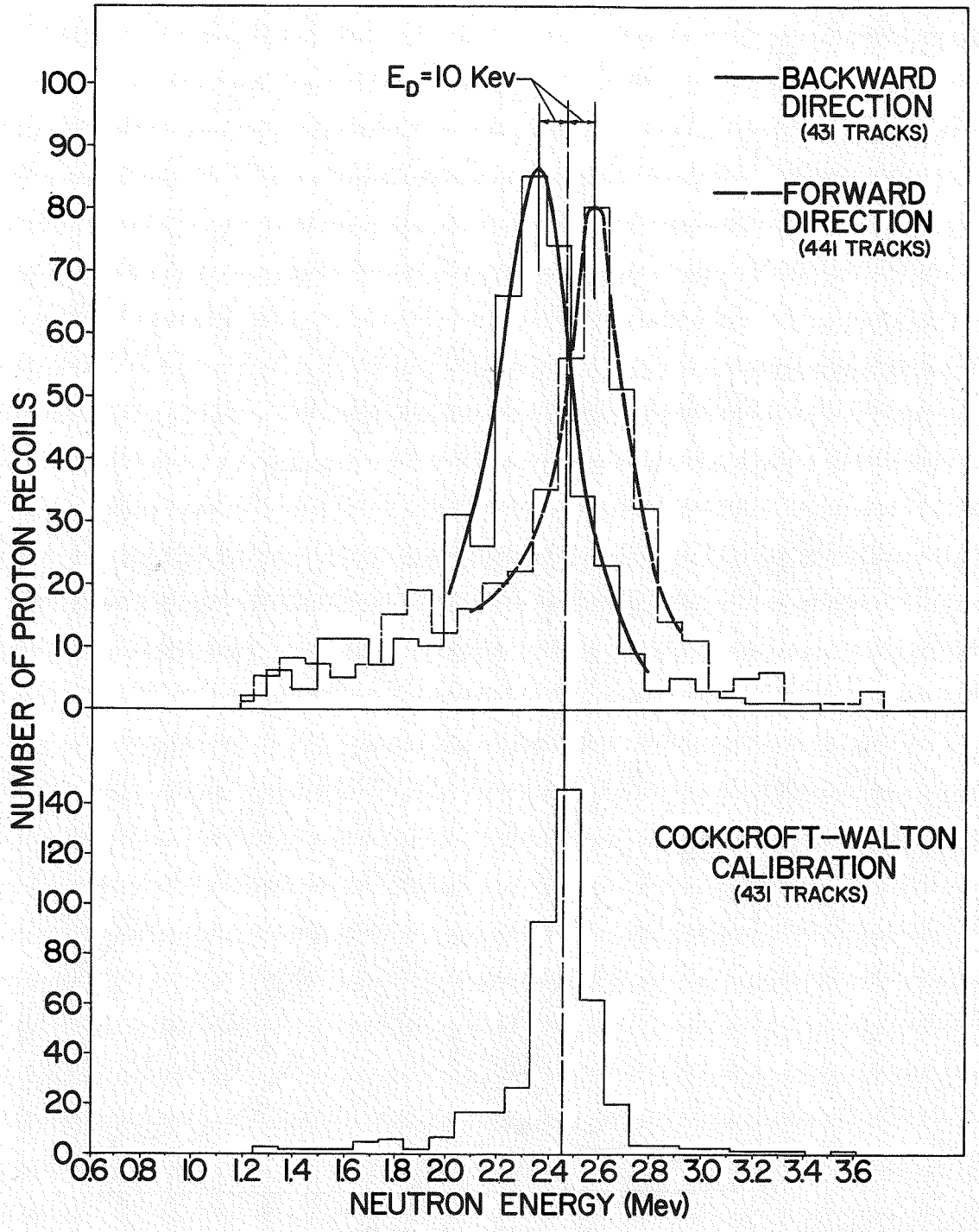

Fig. 10. Neutron energy distributions measured tangentially to the torus circumference in the direction of accelerated deuterons and in a direction opposite to that of the accelerated deuterons. Also pictured is a calibration measurement performed with a mono-energetic source of neutrons from a Cockcroft-Walton accelerator.

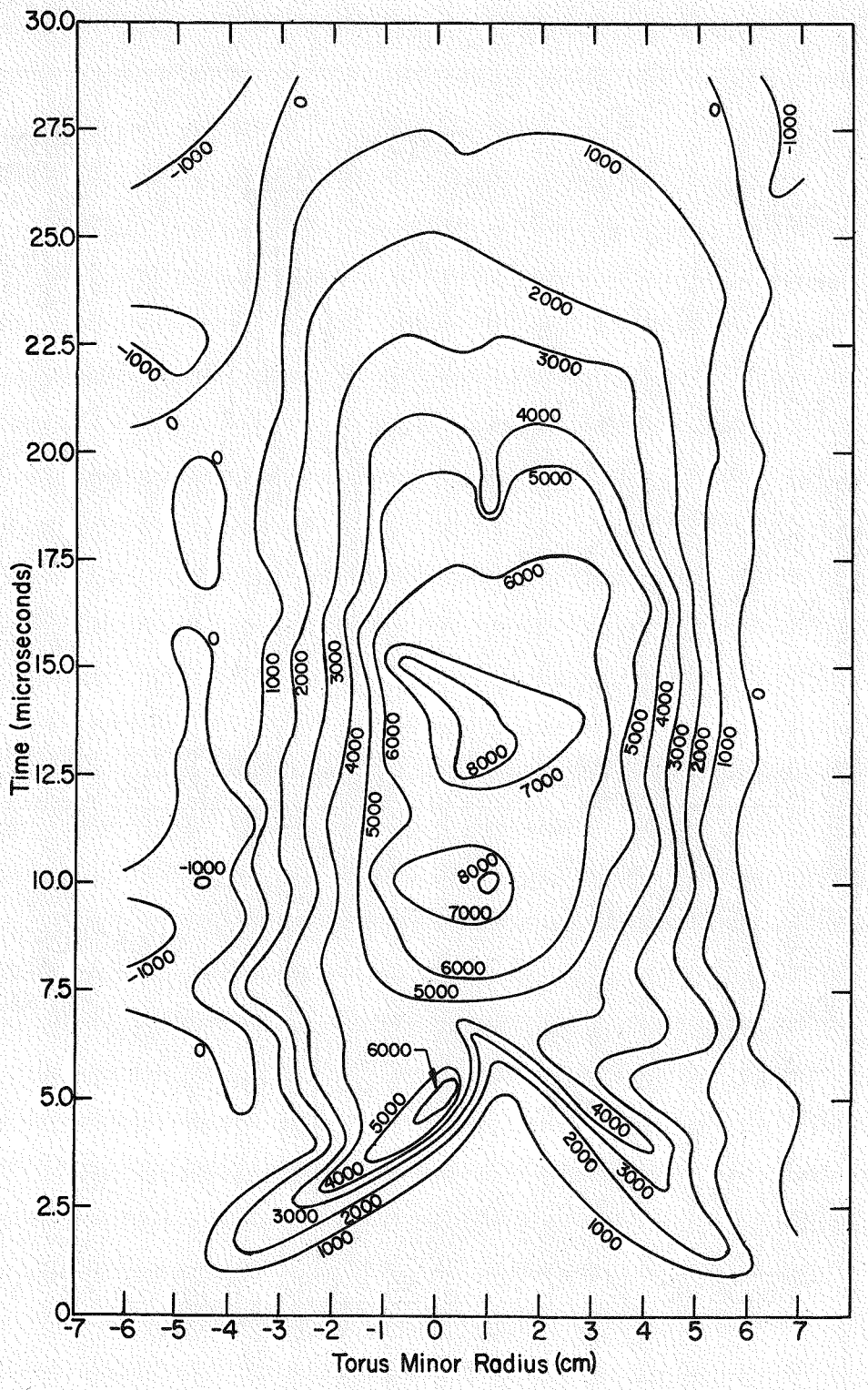

Fig. 11a. Contour plot of axial j_z current density (amperes/cm^2) as a function of radius and time. Operating conditions: primary voltage = 30 kv, axial B_z field = 1700 gauss, P = 12.5 microns.

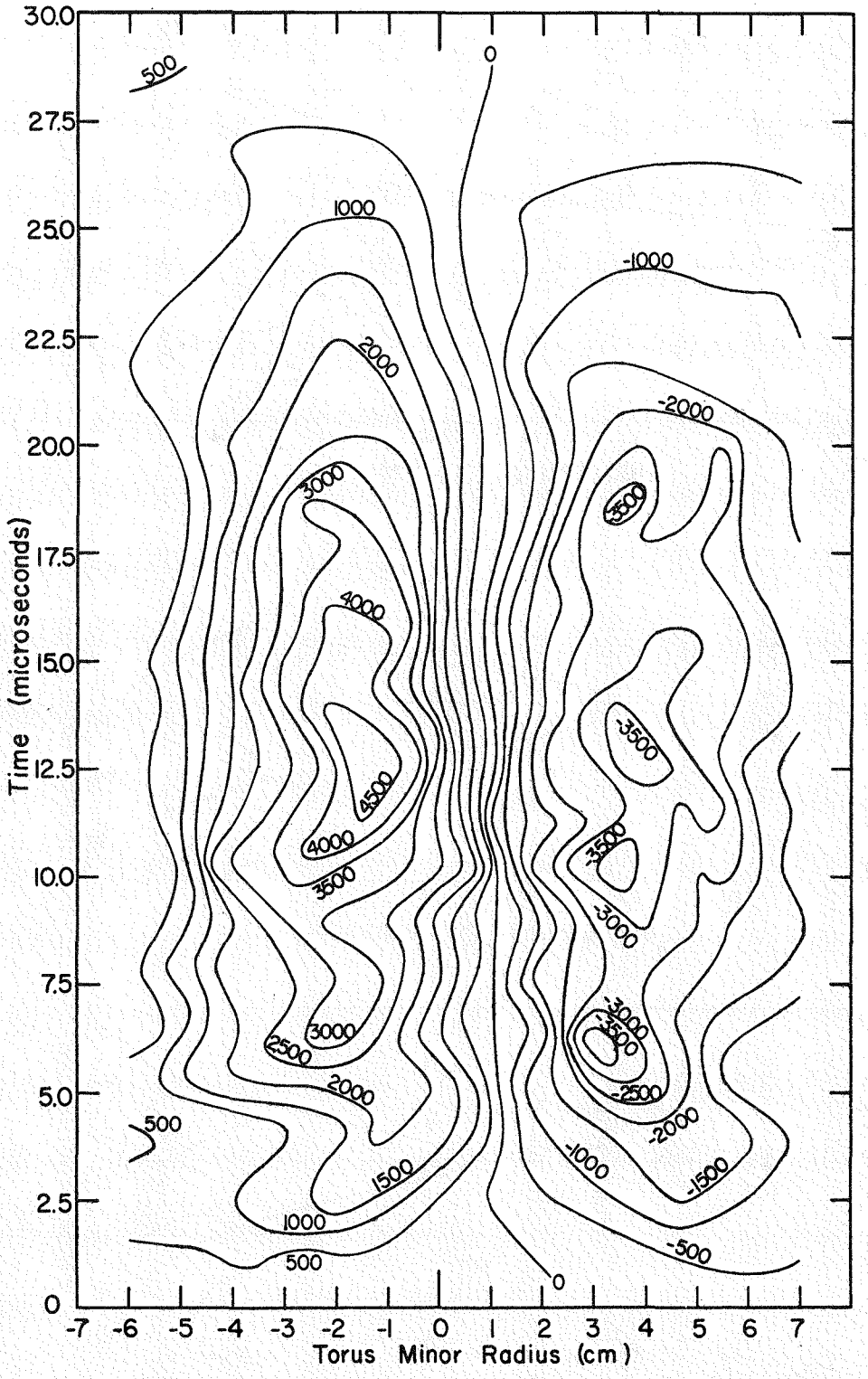

Fig. 11b. Contour plot of transverse j_θ current density (amperes/cm^2) as a function of radius and time. Operating conditions: primary voltage = 30 kv, axial B_z field = 1700 gauss, P = 12.5 microns.

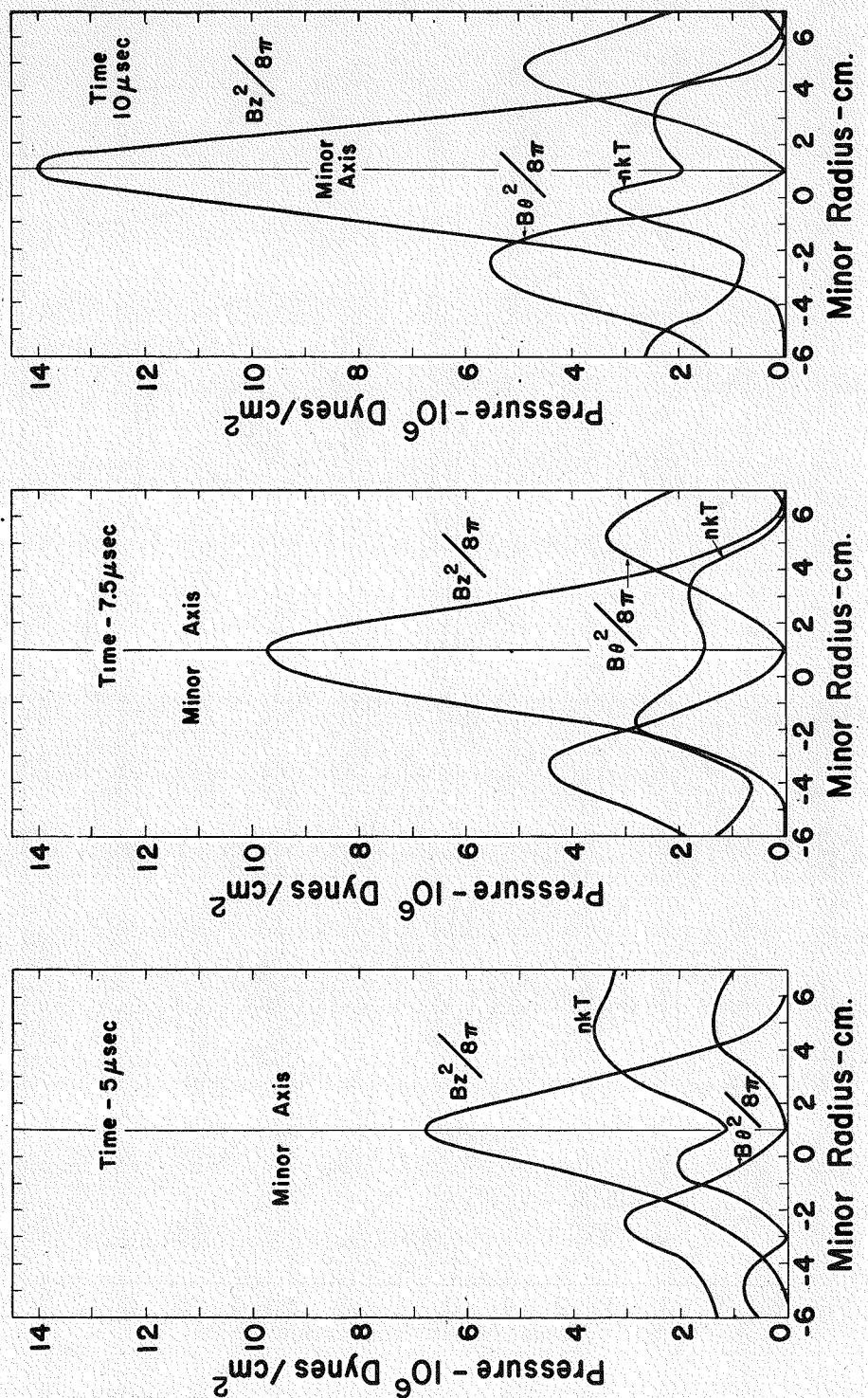

Fig. 12. Calculated pressure distributions as a function of radius at t = 5.0, 7.5, and 10.0 μsec.

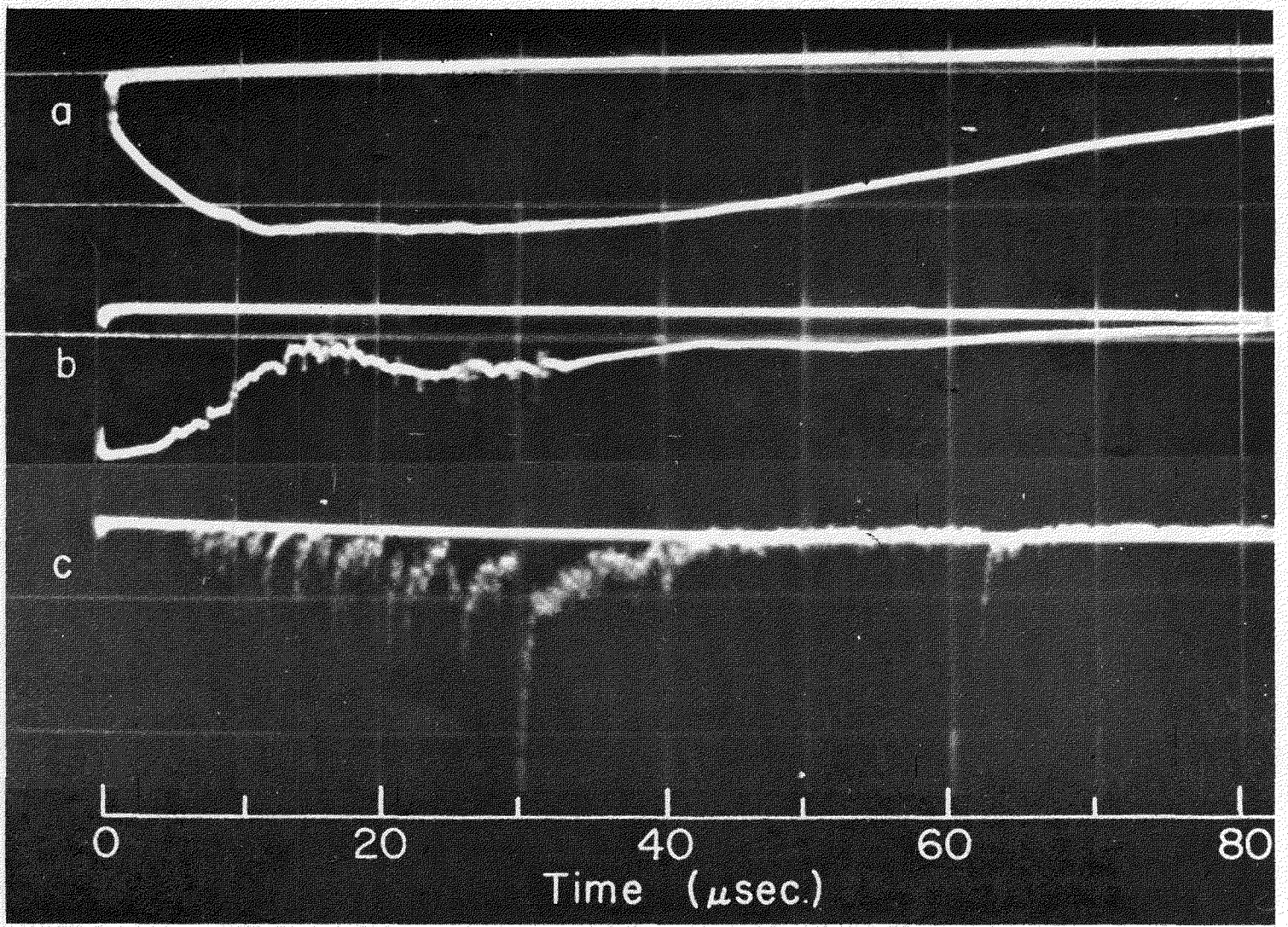

Fig. 13. Multibeam oscilloscope traces of sustained crowbar operation: (a) gas discharge current, (b) secondary voltage, (c) neutron emission. Primary voltage = 14 kv, sustained crowbar voltage = 6 kv, B_z field = 700 gauss.

A/CONF.15/P/2488
USA

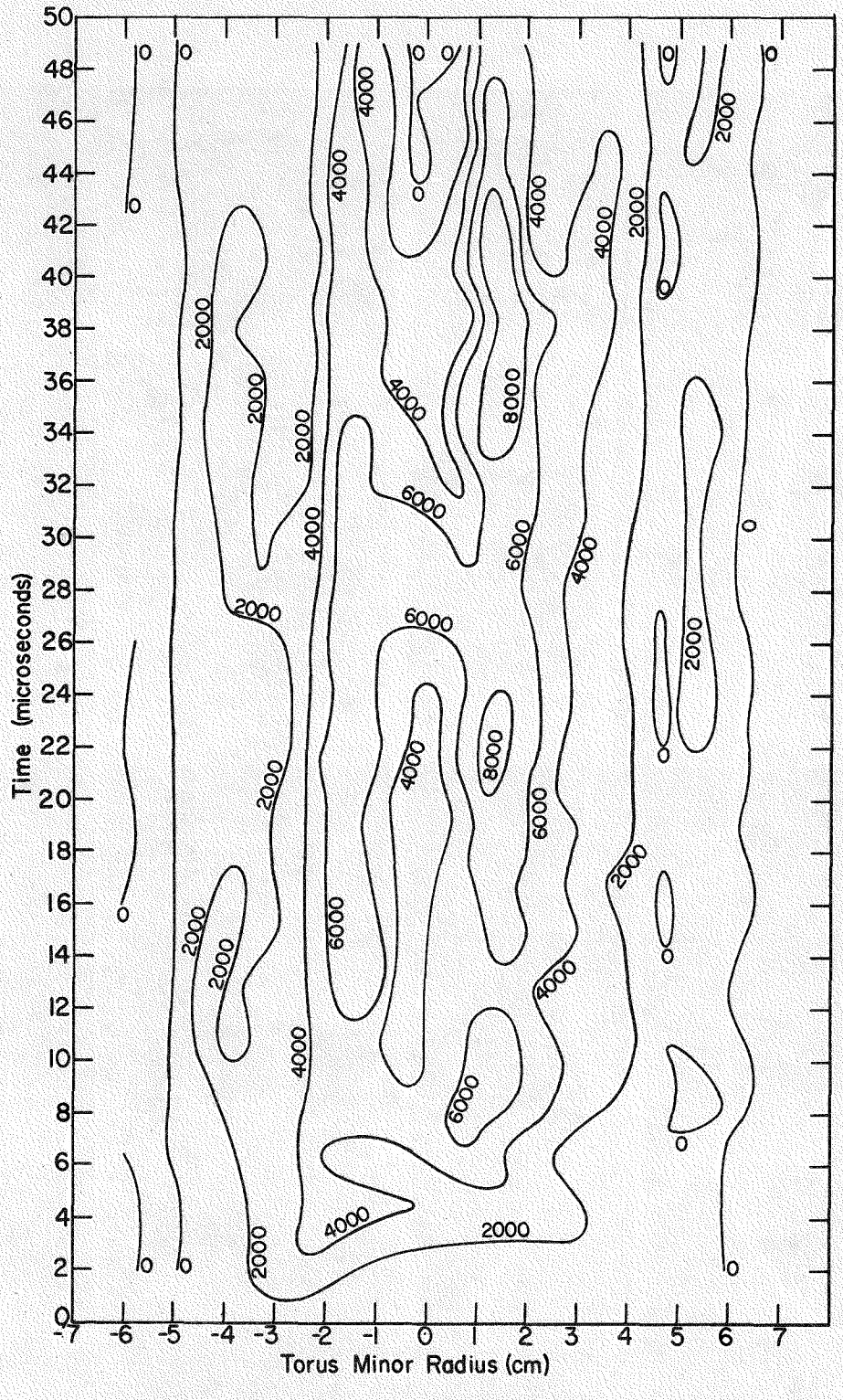

Fig. 14a. Contour plot of axial j_z current density (amperes/cm^2) as a function of time and radius for sustained crowbar operation. Primary voltage = 14 kv, sustained crowbar voltage = 6 kv, B_z field = 700 gauss, and P = 12.5 microns.

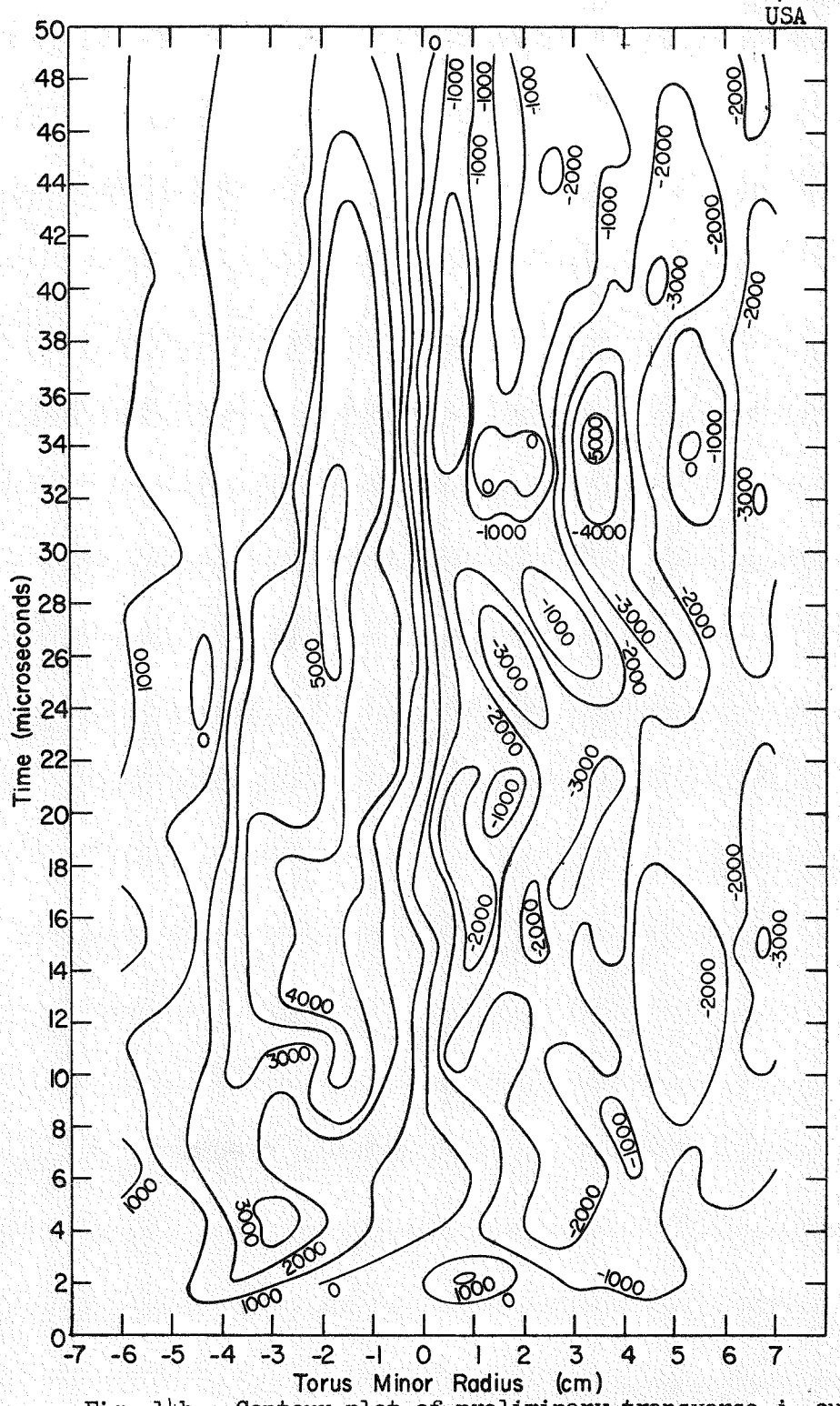

Fig. 14b. Contour plot of preliminary transverse j_θ current density (amperes/cm^2) data as a function of radius and time for sustained crowbar operation. Primary voltage = 14 kv, sustained crowbar voltage = 6 kv, B_z field = 700 gauss, and P = 12.5 microns.

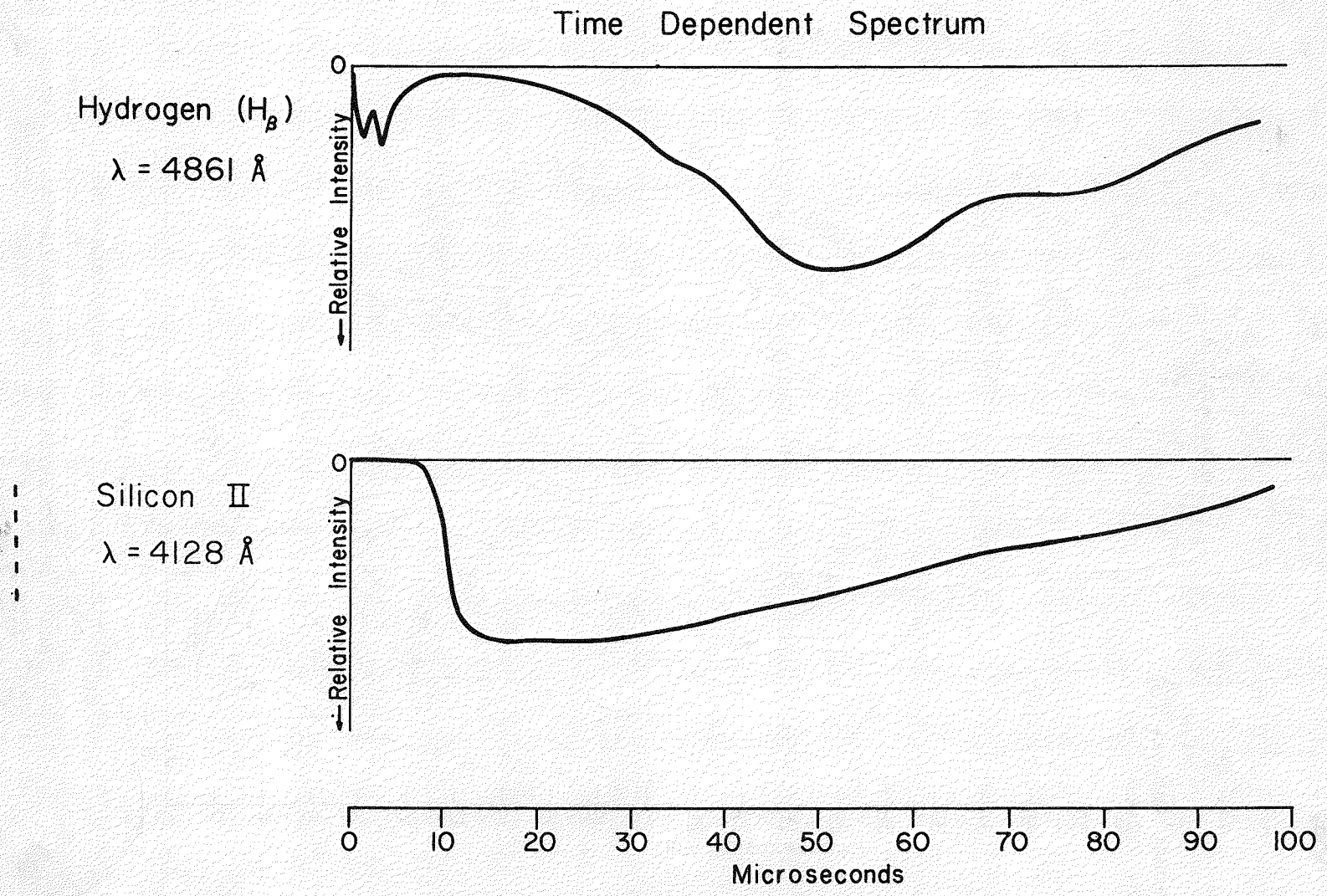

Fig. 15. Intensity distribution of deuterium (D_β, 4861 Å) and Si II (4128Å) light as a function of time. Primary voltage = 30 kv, axial B_z field = 1700 gauss, P = 12.5 microns.